

Higgs Mass Bounds, Type II SeeSaw and LHC

Ilia Gogoladze^{a,1}, Nobuchika Okada^{b,2} and Qaisar Shafi^{a,3}

^a*Bartol Research Institute, Department of Physics and Astronomy,
University of Delaware, Newark, DE 19716, USA*

^b*Theory Division, KEK, Tsukuba 305-0801, Japan*

Abstract

In type II seesaw utilized to explain the observed neutrino masses and mixings, one extends the Standard Model (SM) by introducing scalar fields which transform as a triplet under the electroweak gauge symmetry. New scalar couplings involving the Higgs doublet then appear and, as we show, these have important implications for the Higgs boson mass bounds obtained using vacuum stability and perturbativity arguments. We identify, in particular, regions of the parameter space which permit the SM Higgs boson to be as light as 114.4 GeV, the LEP2 bound. The triplet scalars include doubly charged particles whose masses could, in principle, be in the few hundred GeV range, and so they may be accessible at the LHC.

¹ E-mail: ilia@physics.udel.edu

² E-mail: okadan@post.kek.jp

³ E-mail: shafi@bartol.udel.edu

The discovery of the Standard Model (SM) Higgs boson is arguably the single most important mission for the LHC. Under the somewhat radical assumption that the next energy frontier lies at Planck scale (M_{Pl}), it has been found that the SM Higgs boson mass lies in the range $127 \text{ GeV} \leq M_H \leq 170 \text{ GeV}$ [1]. Here the lower bound of 127 GeV on M_H derives from arguments based on the stability of the SM vacuum (more precisely, that the Higgs quartic coupling does not turn negative at any scale between M_Z and M_{Pl}). Thus, from the point of view of the SM it is perhaps not too surprising that the Higgs boson has not yet been found. The upper bound of about 170 GeV on M_H comes from the requirement that the Higgs quartic coupling remains perturbative and does not exceed $\sqrt{4\pi}$, say, during its evolution between M_Z and M_{Pl} .

It has become abundantly clear in recent years that an extension of the SM is needed to explain a number of experimental observations. These include solar and atmospheric neutrino oscillations [2], existence of non-baryonic dark matter [3], the observed baryon asymmetry of the universe, etc. Neutrino oscillations, in particular, cannot be understood within the SM, even after including dimension five operators with Planck scale cutoff. These operators yield neutrino masses of order 10^{-5} eV or less, which is far below the 0.05-0.01 eV scale needed to explain the observed atmospheric and solar neutrino oscillations, respectively.

Two attractive seesaw mechanisms exist for explaining the measured neutrino masses (more accurately, mass differences squared). In the so-called type I seesaw [4], new physics is added to the SM by introducing at least two heavy right-handed neutrinos. The seesaw mechanism then ensures that the observed neutrinos acquire masses which are suppressed by the heavy right-handed neutrino mass scale(s). One expects that the heaviest right-handed neutrino has a mass less than or of order 10^{14} GeV (This, roughly speaking, comes from the seesaw formula m_D^2/M_R for the light neutrino mass, where m_D and M_R denote the Dirac and right-handed neutrino masses, respectively, and assumes that m_D is less than or of order the electroweak scale).

In type II seesaw [5], the SM is supplemented by a $SU(2)_L$ triplet scalar field Δ which also carries unit hypercharge. There exist renormalizable couplings $\ell^T \Delta \ell$ which enable the neutrinos to acquire their tiny (observed) masses through the non-zero VEV of Δ .

From our point of view one of the most interesting features in type II seesaw derives from the fact that the $SU(2)_L$ triplet Δ interacts with the SM Higgs doublet via both cubic and quartic scalar couplings. These, as we will show in this letter, can have far reaching implications for the SM bounds on M_H , which can be studied by employing the coupled renormalization group equations(RGEs) involving the SM Higgs doublet ϕ and Δ . We find, in particular, that for a plausible choice of parameters, the SM Higgs boson mass M_H can be as low as the LEP2 bound

of 114.4 GeV.

This is in sharp contrast with type I seesaw in which the lower bound of 127 GeV for M_H is increased by the presence of Dirac Yukawa coupling(s) involving right-handed neutrinos [6]. With a Dirac Yukawa coupling equal, say, to unity, the vacuum stability bound is increased to 156 GeV, while the perturbativity bound remains close to 170 GeV. The key difference is that in type II seesaw a mass for the SM Higgs boson, say in the range of 115 - 127 GeV, is easily realized, which is not the case for type I seesaw.

Before moving to the technical part let us note that Δ contains doubly charged particles which, if not too heavy, may be produced at the LHC and Tevatron [7]. It is amusing that with type II seesaw, a 'light' SM Higgs is consistent with relatively light Δ particles with masses around a few hundred GeV. Of course, it may turn out that the mass scale for Δ lies well above the TeV range, in which case we will only find the 'light' Higgs boson at the LHC.

We begin by introducing a triplet Higgs scalar Δ , which transforms as $(\mathbf{3}, 1)$ under the electroweak gauge group $SU(2)_L \times U(1)_Y$:

$$\Delta = \frac{\sigma^i}{\sqrt{2}} \Delta_i = \begin{pmatrix} \Delta^+/\sqrt{2} & \Delta^{++} \\ \Delta^0 & -\Delta^+/\sqrt{2} \end{pmatrix}. \quad (1)$$

The scalar potential involving both the SM Higgs doublet and the triplet Higgs is given by (throughout this paper, we follow the notation of Ref. [8], except that we employ lower case Greek letters for dimensionless couplings)

$$\begin{aligned} V(\Delta, \phi) = & -m_\phi^2(\phi^\dagger\phi) + \frac{\lambda}{2}(\phi^\dagger\phi)^2 \\ & + M_\Delta^2 \text{tr}(\Delta^\dagger\Delta) + \frac{\lambda_1}{2}(\text{tr}\Delta^\dagger\Delta)^2 + \frac{\lambda_2}{2} \left[(\text{tr}\Delta^\dagger\Delta)^2 - \text{tr}(\Delta^\dagger\Delta\Delta^\dagger\Delta) \right] \\ & + \lambda_4 \phi^\dagger\phi \text{tr}(\Delta^\dagger\Delta) + \lambda_5 \phi^\dagger [\Delta^\dagger, \Delta] \phi + \left[\frac{\Lambda_6}{\sqrt{2}} \phi^T i\sigma_2 \Delta^\dagger \phi + \text{h.c.} \right], \end{aligned} \quad (2)$$

where ϕ $(\mathbf{2}, 1/2)$ is the SM Higgs doublet. Without loss of generality the coupling constants λ_i are taken to be real through a phase rotation of Δ . Note that we define a dimensionless parameter $\lambda_6 \equiv \Lambda_6/M_\Delta$. The triplet Higgs has a Yukawa coupling with the lepton doublets (ℓ_L^i , with generation index i) of the form,

$$\mathcal{L}_\Delta = -\frac{1}{\sqrt{2}} (Y_\Delta)_{ij} \ell_L^{Ti} C i\sigma_2 \Delta \ell_L^j + \text{h.c.}, \quad (3)$$

where C is the Dirac charge conjugate matrix and $(Y_\Delta)_{ij}$ denotes elements of the Yukawa matrix.

Assuming the hierarchy $M_Z \ll M_\Delta$ and integrating out the heavy triplet Higgs, we obtain a low energy effective potential for the SM doublet,

$$V(\phi)_{\text{eff}} = -m_\phi^2(\phi^\dagger\phi) + \frac{1}{2}(\lambda - \lambda_6^2)(\phi^\dagger\phi)^2. \quad (4)$$

Below M_Δ the SM Higgs quartic coupling is given by [9]

$$\lambda_{\text{SM}} = \lambda - \lambda_6^2. \quad (5)$$

For a given λ_6 , the Higgs quartic coupling is shifted down to the SM coupling by λ_6^2 through this matching condition at $\mu = M_\Delta$, so that the resulting Higgs boson mass, as we will show, is lowered.

A non-zero VEV ($v = 246.2$ GeV) for the Higgs doublet induces a tadpole term for Δ via the last term in Eq. (2). A non-zero VEV of the triplet Higgs is thereby generated, $\langle \Delta \rangle \sim \lambda_6 v^2 / M_\Delta$, which then provides the desired neutrino masses using Eq. (3).

Note that the triplet Higgs VEV contributes to the weak boson masses and alters the ρ -parameter from the SM prediction, $\rho \approx 1$, at tree level. The current precision measurement [10] constrains this deviation to be in the range, $\Delta\rho = \rho - 1 \simeq \langle \Delta \rangle / v \lesssim 0.01$, so that $\lambda_6 \lesssim 0.01 M_\Delta / v$. This constraint is especially relevant when we consider $M_\Delta \sim \text{TeV}$, in which case the region $\lambda_6 \gtrsim 0.1$ is excluded.

We are now ready to analyze the Higgs boson mass bounds from vacuum stability and perturbativity constraints in the presence of type II seesaw mechanism. There are several new parameters $\lambda_1, \lambda_2, \lambda_4, \lambda_5, \lambda_6$, and Y_Δ , which potentially affect the RGE running of the Higgs quartic coupling and thus the corresponding Higgs boson mass. We have already noted the important role that λ_6 plays via the matching condition in Eq. (5). It turns out that both λ_4 and λ_5 will also play an important role through their contributions to the renormalization group evolution of the Higgs quartic coupling. They help to lower both the vacuum stability and perturbativity bounds on the SM Higgs mass. In our analysis, we employ two-loop RGEs for the SM couplings and one-loop RGEs for the new couplings associated with the type II seesaw scenario.

For renormalization scale $\mu < M_\Delta$, the triplet Higgs is decoupled. For the three SM gauge couplings, we have

$$\frac{dg_i}{d \ln \mu} = \frac{b_i}{16\pi^2} g_i^3 + \frac{g_i^3}{(16\pi^2)^2} \sum_{j=1}^3 b_{ij} g_j^2, \quad (6)$$

where g_i ($i = 1, 2, 3$) are the SM gauge couplings and

$$b_i = \left(\frac{41}{10}, -\frac{19}{6}, -7 \right), \quad b_{ij} = \begin{pmatrix} \frac{199}{50} & \frac{27}{10} & \frac{44}{5} \\ \frac{9}{10} & \frac{35}{6} & 12 \\ \frac{11}{10} & \frac{9}{2} & -26 \end{pmatrix}. \quad (7)$$

The top quark pole mass is taken to be the central value $M_t = 170.9$ GeV, [11], with $(\alpha_1, \alpha_2, \alpha_3) = (0.01681, 0.03354, 0.1176)$ at the Z-pole (M_Z) [10]. For the top Yukawa coupling y_t , we have

[12],

$$\frac{dy_t}{d \ln \mu} = y_t \left(\frac{1}{16\pi^2} \beta_t^{(1)} + \frac{1}{(16\pi^2)^2} \beta_t^{(2)} \right). \quad (8)$$

Here the one-loop contribution is

$$\beta_t^{(1)} = \frac{9}{2} y_t^2 - \left(\frac{17}{20} g_1^2 + \frac{9}{4} g_2^2 + 8g_3^2 \right), \quad (9)$$

while the two-loop contribution is given by

$$\begin{aligned} \beta_t^{(2)} = & -12y_t^4 + \left(\frac{393}{80} g_1^2 + \frac{225}{16} g_2^2 + 36g_3^2 \right) y_t^2 \\ & + \frac{1187}{600} g_1^4 - \frac{9}{20} g_1^2 g_2^2 + \frac{19}{15} g_1^2 g_3^2 - \frac{23}{4} g_2^4 + 9g_2^2 g_3^2 - 108g_3^4 \\ & + \frac{3}{2} \lambda^2 - 6\lambda y_t^2. \end{aligned} \quad (10)$$

In solving Eq. (8), the initial top Yukawa coupling at $\mu = M_t$ is determined from the relation between the pole mass and the running Yukawa coupling [13], [14],

$$M_t \simeq m_t(M_t) \left(1 + \frac{4}{3} \frac{\alpha_3(M_t)}{\pi} + 11 \left(\frac{\alpha_3(M_t)}{\pi} \right)^2 - \left(\frac{m_t(M_t)}{2\pi v} \right)^2 \right), \quad (11)$$

with $y_t(M_t) = \sqrt{2}m_t(M_t)/v$, where $v = 246.2$ GeV. Here, the second and third terms in the parenthesis correspond to one- and two-loop QCD corrections, respectively, while the fourth term comes from the electroweak corrections at one-loop level. The numerical values of the third and fourth terms are comparable (signs are opposite). The electroweak corrections at two-loop level and the three-loop QCD corrections [14], are of comparable and sufficiently small magnitude [14] to be safely ignored.

The RGE for the Higgs quartic coupling is given by [12],

$$\frac{d\lambda}{d \ln \mu} = \frac{1}{16\pi^2} \beta_\lambda^{(1)} + \frac{1}{(16\pi^2)^2} \beta_\lambda^{(2)}, \quad (12)$$

with

$$\begin{aligned} \beta_\lambda^{(1)} = & 12\lambda^2 - \left(\frac{9}{5} g_1^2 + 9g_2^2 \right) \lambda + \frac{9}{4} \left(\frac{3}{25} g_1^4 + \frac{2}{5} g_1^2 g_2^2 + g_2^4 \right) \\ & + 12y_t^2 \lambda - 12y_t^4, \end{aligned} \quad (13)$$

and

$$\begin{aligned} \beta_\lambda^{(2)} = & -78\lambda^3 + 18 \left(\frac{3}{5} g_1^2 + 3g_2^2 \right) \lambda^2 - \left(\frac{73}{8} g_2^4 - \frac{117}{20} g_1^2 g_2^2 + \frac{2661}{100} g_1^4 \right) \lambda - 3\lambda y_t^4 \\ & + \frac{305}{8} g_2^6 - \frac{289}{40} g_1^2 g_2^4 - \frac{1677}{200} g_1^4 g_2^2 - \frac{3411}{1000} g_1^6 - 64g_3^2 y_t^4 - \frac{16}{5} g_1^2 y_t^4 - \frac{9}{2} g_2^4 y_t^2 \\ & + 10\lambda \left(\frac{17}{20} g_1^2 + \frac{9}{4} g_2^2 + 8g_3^2 \right) y_t^2 - \frac{3}{5} g_1^2 \left(\frac{57}{10} g_1^2 - 21g_2^2 \right) y_t^2 - 72\lambda^2 y_t^2 + 60y_t^6. \end{aligned} \quad (14)$$

The Higgs boson pole mass M_H is determined by the relation to the running Higgs quartic coupling through the one-loop matching condition [15] ,

$$\lambda(M_H) v^2 = M_H^2 (1 + \Delta_h(M_H)) , \quad (15)$$

where

$$\Delta_h(M_H) = \frac{G_F}{\sqrt{2}} \frac{M_Z^2}{16\pi^2} \left[\frac{M_H^2}{M_Z^2} f_1 \left(\frac{M_H^2}{M_Z^2} \right) + f_0 \left(\frac{M_H^2}{M_Z^2} \right) + \frac{M_Z^2}{M_H^2} f_{-1} \left(\frac{M_H^2}{M_Z^2} \right) \right] \quad (16)$$

The functions are given by

$$\begin{aligned} f_1(\xi) &= \frac{3}{2} \ln \xi - \frac{1}{2} Z \left(\frac{1}{\xi} \right) - Z \left(\frac{c_w^2}{\xi} \right) - \ln c_w^2 + \frac{9}{2} \left(\frac{25}{9} - \frac{\pi}{\sqrt{3}} \right) , \\ f_0(\xi) &= -6 \ln \frac{M_H^2}{M_Z^2} \left[1 + 2c_w^2 - 2 \frac{M_t^2}{M_Z^2} \right] + \frac{3c_w^2 \xi}{\xi - c_w^2} \ln \frac{\xi}{c_w^2} + 2Z \left(\frac{1}{\xi} \right) \\ &\quad + 4c_w^2 Z \left(\frac{c_w^2}{\xi} \right) + \left(\frac{3c_w^2}{s_w^2} + 12c_w^2 \right) \ln c_w^2 - \frac{15}{2} (1 + 2c_w^2) \\ &\quad - 3 \frac{M_t^2}{M_Z^2} \left[2Z \left(\frac{M_t^2}{M_Z^2 \xi} \right) + 4 \ln \frac{M_t^2}{M_Z^2} - 5 \right] , \\ f_{-1}(\xi) &= 6 \ln \frac{M_H^2}{M_Z^2} \left[1 + 2c_w^4 - 4 \frac{M_t^4}{M_Z^4} \right] - 6Z \left(\frac{1}{\xi} \right) - 12c_w^4 Z \left(\frac{c_w^2}{\xi} \right) - 12c_w^4 \ln c_w^2 \\ &\quad + 8 (1 + 2c_w^4) + 24 \frac{M_t^4}{M_Z^4} \left[\ln \frac{M_t^2}{M_Z^2} - 2 + Z \left(\frac{M_t^2}{M_Z^2 \xi} \right) \right] , \end{aligned} \quad (17)$$

with $s_w^2 = \sin^2 \theta_W$, $c_w^2 = \cos^2 \theta_W$ (θ_W denotes the weak mixing angle) and

$$Z(z) = \begin{cases} 2A \arctan(1/A) & (z > 1/4) \\ A \ln [(1+A)/(1-A)] & (z < 1/4), \end{cases} \quad (18)$$

with $A = \sqrt{|1 - 4z|}$.

For $\mu \geq M_\Delta$, the triplet Higgs contributes to the one-loop RGEs. Consequently, we replace b_i in Eq. (7) with

$$b_i = \left(\frac{47}{10}, -\frac{5}{2}, -7 \right) . \quad (19)$$

The RGE for the top Yukawa coupling is unchanged.

The RGEs for the new couplings in Eqs. (2) and (3) have been calculated in Ref. [16] and more recently in Ref. [8]. The RGE of the Higgs quartic coupling acquires a new entry in Eq.(13),

$$\beta_\lambda^{(1)} \rightarrow \beta_\lambda^{(1)} + 6\lambda_4^2 + 4\lambda_5^2. \quad (20)$$

Note that in Eq. (20) the contributions from the couplings λ_4 and λ_5 are both positive. This feature will be crucial in lowering both the vacuum stability and perturbativity bounds with type II seesaw.

For the remaining couplings we have [8],

$$16\pi^2 \frac{d\lambda_1}{d\ln\mu} = -\left(\frac{36}{5}g_1^2 + 24g_2^2\right)\lambda_1 + \frac{108}{25}g_1^4 + 18g_2^4 + \frac{72}{5}g_1^2g_2^2 + 14\lambda_1^2 + 4\lambda_1\lambda_2 + 2\lambda_2^2 + 4\lambda_4^2 + 4\lambda_5^2 + 4\text{tr}[\mathbf{S}_\Delta]\lambda_1 - 8\text{tr}[\mathbf{S}_\Delta^2], \quad (21)$$

$$16\pi^2 \frac{d\lambda_2}{d\ln\mu} = -\left(\frac{36}{5}g_1^2 + 24g_2^2\right)\lambda_2 + 12g_2^4 - \frac{144}{5}g_1^2g_2^2 + 3\lambda_2^2 + 12\lambda_1\lambda_2 - 8\lambda_5^2 + 4\text{tr}[\mathbf{S}_\Delta]\lambda_2 + 8\text{tr}[\mathbf{S}_\Delta^2], \quad (22)$$

$$16\pi^2 \frac{d\lambda_4}{d\ln\mu} = -\left(\frac{9}{2}g_1^2 + \frac{33}{2}g_2^2\right)\lambda_4 + \frac{27}{25}g_1^4 + 6g_2^4 + (8\lambda_1 + 2\lambda_2 + 6\lambda + 4\lambda_4 + 6y_t^2 + 2\text{tr}[\mathbf{S}_\Delta])\lambda_4 + 8\lambda_5^2 - 4\text{tr}[\mathbf{S}_\Delta^2], \quad (23)$$

$$16\pi^2 \frac{d\lambda_5}{d\ln\mu} = -\frac{9}{2}g_1^2\lambda_5 - \frac{33}{2}g_2^2\lambda_5 - \frac{18}{5}g_1^2g_2^2 + (2\lambda_1 - 2\lambda_2 + 2\lambda + 8\lambda_4 + 6y_t^2 + 2\text{tr}[\mathbf{S}_\Delta])\lambda_5 + 4\text{tr}[\mathbf{S}_\Delta^2]. \quad (24)$$

Here, $\mathbf{S}_\Delta = Y_\Delta^\dagger Y_\Delta$ and its corresponding RGE is given by

$$16\pi^2 \frac{d\mathbf{S}_\Delta}{d\ln\mu} = 6\mathbf{S}_\Delta^2 - 3\left(\frac{3}{5}g_1^2 + 3g_2^2\right)\mathbf{S}_\Delta + 2\text{tr}[\mathbf{S}_\Delta]\mathbf{S}_\Delta. \quad (25)$$

In our analysis, we do not consider the RGE for λ_6 because, at one-loop level, it is decoupled from the other RGEs. We assume though that like all other couplings, it remains in the perturbative region throughout. However, note that λ_6 plays an important role in our analysis through the matching condition for the Higgs quartic coupling between high and low energies. The SM Higgs quartic coupling as the low energy effective coupling is defined in Eq. (5). Therefore, the RGE solution of the SM Higgs quartic coupling is connected to the solution for the Higgs quartic coupling at high energies through the matching condition at $\mu = M_\Delta$ [9]. For a given λ_6 , the Higgs quartic coupling is shifted down to the SM coupling by λ_6^2 through this matching condition at $\mu = M_\Delta$, so that the resulting Higgs boson mass is lowered.

Next we analyze the RGEs numerically and show how much the vacuum stability and perturbativity bounds on Higgs boson mass are altered in the presence of type II seesaw. In addition to the matching condition, $\lambda_{4,5}$ have important effects on the running of the Higgs quartic coupling since they appear in Eq. (20). Their contributions are positive and these couplings work so as to reduce the Higgs quartic coupling at low energies. Consequently, we can expect that the resultant Higgs boson mass tends to be reduced from the effects of λ_6 and $\lambda_{4,5}$ in type II seesaw. Although the other parameters $\lambda_{1,2}$ and Y_Δ are not involved in the RGE

of Higgs quartic coupling, they, of course, do affect the Higgs boson mass through their RGEs coupled with $\lambda_{4,5}$. To keep the discussion as simple as possible we proceed as follows. We first investigate the Higgs boson mass bounds by varying λ_6 , while keeping the other(non-SM) parameters fixed. We show that a Higgs mass as low as the LEP 2 bound can be realized in this case. With the seesaw scale at TeV, however, the lower bound on the Higgs mass is closer to 120 GeV. For our next examples we vary λ_5 , keeping the other(non-SM) parameters fixed. This case yields a lower bound of 114.4 GeV for the Higgs boson mass which is compatible with a low (TeV or so) seesaw scale.

Fixing the cutoff scale as $M_{Pl} = 1.2 \times 10^{19}$ GeV, we define the vacuum stability bound as the lowest Higgs mass given by the running Higgs quartic coupling which satisfies the condition $\lambda(\mu) \geq 0$ for any scale between $M_H \leq \mu \leq M_{Pl}$. On the other hand, the perturbativity bound is defined as the highest Higgs boson mass given by the running Higgs quartic coupling which satisfies the condition $\lambda(\mu) \leq \sqrt{4\pi}$ for any scale between $M_H \leq \mu \leq M_{Pl}$.

In Fig. 1, the running Higgs mass defined as $\sqrt{\lambda(\mu)}v$ for the vacuum stability bound is depicted for various λ_6 and a fixed seesaw scale $M_\Delta = 10^{12}$ GeV. Here we took simple inputs as $\lambda_1 = \sqrt{4\pi}$, $\lambda_2 = -1$, $\lambda_4 = \lambda_5 = 0$ and $Y_\Delta = 0$. Fig. 2 shows a running Higgs mass for the perturbativity bound for various λ_6 with the same inputs for the other parameters as in Fig. 1. We find that as λ_6 is increased, the vacuum stability and perturbativity bounds eventually merge. The corresponding Higgs mass coincides, it turns out, with the vacuum stability bound for the SM Higgs boson mass obtained with a cutoff scale $\Lambda = M_\Delta$.

In other words, the window for the Higgs boson mass between the vacuum stability and perturbative bounds becomes narrow and is eventually closed as λ_6 becomes sufficiently large. Fig. 3 shows the window for the Higgs boson pole mass versus λ_6 for various M_Δ . For a suitable choice of λ_6 and M_Δ , values for M_H close to the LEP2 bound are easily realized. Note that with M_Δ of order a TeV or so, the lower bound on the Higgs mass is close to 120 GeV, which is still well below the standard value of 127 GeV in the absence of type II seesaw.

In Fig. 4, a running Higgs mass defined as $\sqrt{\lambda(\mu)}v$ for the vacuum stability bound is depicted for various λ_5 and a fixed seesaw scale $M_\Delta = 10^{12}$ GeV. Here we took sample inputs as $\lambda_1 = \sqrt{4\pi}$, $\lambda_2 = -1$, $\lambda_4 = 0$, $\lambda_6 = 0$ and $Y_\Delta = 0$. Fig. 5 shows a running Higgs mass for the perturbativity bound for various λ_5 with the same inputs for the other parameters as in Fig. 4. This time we find that as λ_5 is raised, the vacuum stability and perturbativity bounds eventually merge. The corresponding Higgs mass coincides with the vacuum stability bound for the SM Higgs boson with a cutoff scale $\Lambda = M_\Delta$. Namely, the window for the Higgs boson mass between the vacuum stability and perturbative bounds becomes narrow and is eventually closed when λ_5 becomes sufficiently large. Fig. 6 shows the window for the Higgs boson pole

mass versus λ_5 for various M_Δ . Note that with $M_\Delta = 1$ TeV and λ_5 close to 0.1, the vacuum stability bound for M_H coincides with the LEP2 bound.

Some comments regarding our analysis are in order here. We employ a set of input parameters such that all couplings remain in the perturbative regime for $M_\Delta \leq \mu \leq M_{Pl}$. For example, for an input parameter set, it may happen that $\lambda_{1,2}$ exceed the perturbative regime at a scale $M_\Delta \leq \mu \leq M_{Pl}$. We checked that the sample parameter set used in Fig. 1-6 did not cause such theoretical inconsistency. To reproduce the current neutrino oscillation data through the type II seesaw mechanism, $\lambda_6 Y_\Delta$ should not be zero. A tiny λ_6 would require a very large Y_Δ , which may cause theoretical inconsistency for the RGEs of Λ_i (see Eq. (21)-(24)). For this reason, we do not strictly set $\lambda_6 = 0$ and $Y_\Delta = 0$ in Figs. 1-6. However, we can check that the impact of Y_Δ in Fig. 3 is negligible when $Y_\Delta \leq 0.1$. In Fig. 6, the effects from Y_Δ and λ_6 are negligible with $Y_\Delta, \lambda_6 \leq 0.1$.

In conclusion, we have considered the potential impact of type II seesaw on the vacuum stability and perturbativity bounds on the Higgs boson mass of the SM. There are two main effects that we have considered. One is the tree level matching condition for the SM Higgs quartic coupling induced by the coupling Λ_6 at the seesaw (triplet mass) scale. The implications for the SM Higgs mass are then studied using the appropriate RGEs. In our second set of examples a different coupling, namely λ_5 , plays an essential role, with Λ_6 essentially subdominant. In both cases we have identified regions of the parameter space for which the lower bound on the SM Higgs boson mass lies well below 127 GeV, the value obtained in the absence of type II seesaw. Perhaps the most interesting result from our analysis is that with type II seesaw the SM Higgs boson can have a mass as low as the LEP 2 bound of 114.4 GeV. This can be achieved for plausible values of the parameters and with the mass scale for the triplet in the TeV range. Thus, it is exciting to speculate that the SM Higgs boson, when found at the LHC, may be accompanied by additional scalar fields with some carrying two units of electric charge.

Acknowledgments

This work is supported in part by the DOE Grant # DE-FG02-91ER40626 (I.G. and Q.S.), and the Grant-in-Aid for Scientific Research from the Ministry of Education, Science and Culture of Japan, #18740170 (N.O.).

References

- [1] N. Cabibbo, L. Maiani, G. Parisi and R. Petronzio, Nucl. Phys. B **158**, 295 (1979); P. Q. Hung, Phys. Rev. Lett. **42**, 873 (1979); M.A.B. Beg, C. Panagiotakopoulos and

- A. Sirlin, Phys. Rev. Lett. **52** (1984) 883; K. S. Babu and E. Ma, Phys. Rev. Lett. **55**, 3005 (1985); M. Lindner, Z. Phys. C **31**, 295 (1986); M. Sher, Phys. Rept. **179**, 273 (1989); G. Altarelli and G. Isidori, Phys. Lett. B **337**, 141 (1994); J. A. Casas, J. R. Espinosa and M. Quiros, Phys. Lett. B **342**, 171 (1995); Phys. Lett. B **382**, 374 (1996); J. R. Espinosa and M. Quiros, Phys. Lett. B **353**, 257 (1995).
- [2] B. T. Cleveland *et al.*, Astrophys. J. **496** 505 (1998); Super-Kamiokande Collaboration, Phys. Lett. **B539** 179 (2002); Super-Kamiokande Collaboration, Phys. Rev. **D71** 112005 (2005); M. Maltoni, T. Schwetz, M.A. Tortola, J.W.F. Valle New J.Phys. **6** 122 (2004); A. Bandyopadhyay *et al.*, Phys. Lett. **B608** 115 (2005); G. L. Fogli *et al.*, Prog. Part. Nucl. Phys. **57** 742 (2006).
- [3] C. L. Bennett *et al.* [WMAP Collaboration], Astrophys. J. Suppl. **148**, 1 (2003); D. N. Spergel *et al.* [WMAP Collaboration], Astrophys. J. Suppl. **148**, 175 (2003); D. N. Spergel *et al.* [WMAP Collaboration], Astrophys. J. Suppl. **170**, 377 (2007).
- [4] P. Minkowski, Phys. Lett. B **67**, 421 (1977); T. Yanagida, in *Proceedings of the Workshop on the Unified Theory and the Baryon Number in the Universe* (O. Sawada and A. Sugamoto, eds.), KEK, Tsukuba, Japan, 1979, p. 95; M. Gell-Mann, P. Ramond, and R. Slansky, *Supergravity* (P. van Nieuwenhuizen *et al.* eds.), North Holland, Amsterdam, 1979, p. 315; S. L. Glashow, *The future of elementary particle physics*, in *Proceedings of the 1979 Cargèse Summer Institute on Quarks and Leptons* (M. Lévy *et al.* eds.), Plenum Press, New York, 1980, p. 687; R. N. Mohapatra and G. Senjanović, Phys. Rev. Lett. **44**, 912 (1980).
- [5] G. Lazarides, Q. Shafi and C. Wetterich, Nucl. Phys. **B181**, 287 (1981); R. N. Mohapatra and G. Senjanović, Phys. Rev. **D 23**, 165 (1981); M. Magg and C. Wetterich, Phys. Lett. B **94**, 61 (1980); J. Schechter and J. W. F. Valle, Phys. Rev. D **22**, 2227 (1980).
- [6] J. A. Casas, V. Di Clemente, A. Ibarra and M. Quiros, Phys. Rev. D **62**, 053005 (2000).
- [7] K. Huitu, J. Maalampi, A. Pietila and M. Raidal, Nucl. Phys. B **487**, 27 (1997); E. J. Chun, K. Y. Lee and S. C. Park, Phys. Lett. B **566**, 142 (2003); A. G. Akeroyd and M. Aoki, Phys. Rev. D **72**, 035011 (2005); T. Han, B. Mukhopadhyaya, Z. Si, and K. Wang, Phys. Rev. **D76**, 075013 (2007); J. Garayoa and T. Schwetz, arXiv:0712.1453 [hep-ph]; A. G. Akeroyd, M. Aoki and H. Sugiyama, arXiv:0712.4019 [hep-ph].
- [8] M. A. Schmidt, Phys. Rev. D **76**, 073010 (2007).

- [9] E. Ma and U. Sarkar, Phys. Rev. Lett. **80**, 5716 (1998).
- [10] W. M. Yao *et al.* [Particle Data Group], J. Phys. G **33** (2006) 1.
- [11] [CDF Collaboration], arXiv:hep-ex/0703034.
- [12] M. E. Machacek and M. T. Vaughn, Nucl. Phys. B **222**, 83 (1983); Nucl. Phys. B **236**, 221 (1984); Nucl. Phys. B **249**, 70 (1985); C. Ford, I. Jack and D. R. T. Jones, Nucl. Phys. **B387** (1992) 373, [Erratum-ibid. **B504** (1997) 551]; H. Arason, D. J. Castano, B. Keszthelyi, S. Mikaelian, E. J. Piard, P. Ramond and B. D. Wright, Phys. Rev. D **46**, 3945 (1992); V. D. Barger, M. S. Berger and P. Ohmann, Phys. Rev. D **47**, 1093 (1993); M. X. Luo and Y. Xiao, Phys. Rev. Lett. **90**, 011601 (2003).
- [13] See, for example, H. Arason, D. J. Castano, B. Keszthelyi, S. Mikaelian, E. J. Piard, P. Ramond and B. D. Wright, Phys. Rev. D **46**, 3945 (1992); H. E. Haber, R. Hempfling and A. H. Hoang, Z. Phys. C **75**, 539 (1997).
- [14] See, for example, F. Jegerlehner, M. Y. Kalmykov and O. Veretin, Nucl. Phys. B **641**, 285 (2002); Nucl. Phys. B **658**, 49 (2003); F. Jegerlehner and M. Y. Kalmykov, Nucl. Phys. B **676**, 365 (2004).
- [15] A. Sirlin and R. Zucchini, Nucl. Phys. B **266** (1986) 389.
- [16] W. Chao and H. Zhang, Phys. Rev. D **75**, 033003 (2007).
- [17] R. Barate *et al.* [LEP Working Group for Higgs boson searches], Phys. Lett. B **565**, 61 (2003).

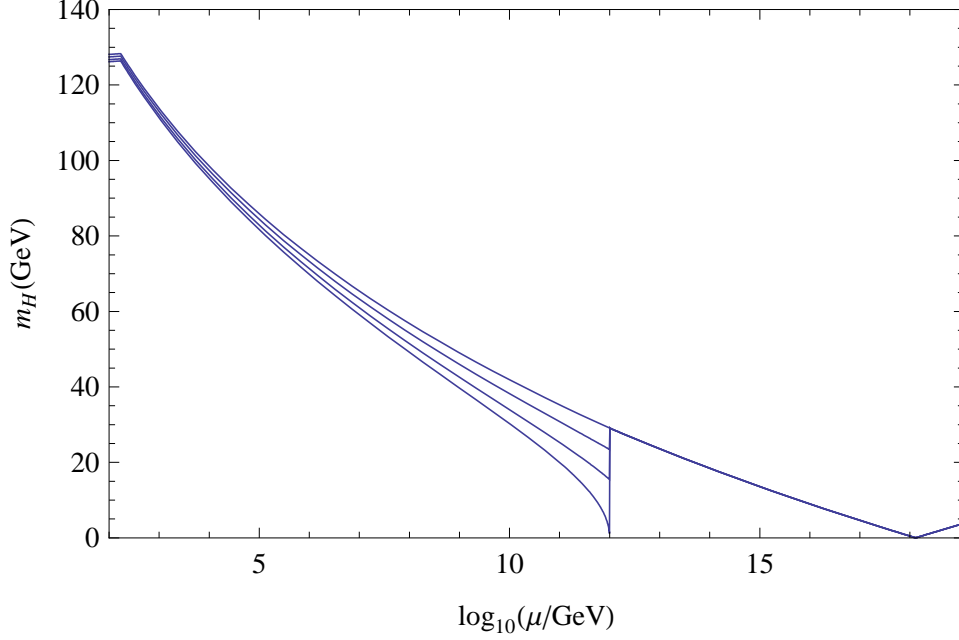


Figure 1: Evolution of running Higgs boson mass ($m_h(\mu = \sqrt{\lambda(\mu)}v)$) corresponding to the vacuum stability bound for various λ_6 and $M_\Delta = 10^{12}$ GeV . Each line corresponds to $\lambda_6 = 0, 0.07, 0.1$ and 0.118 , from top to bottom.

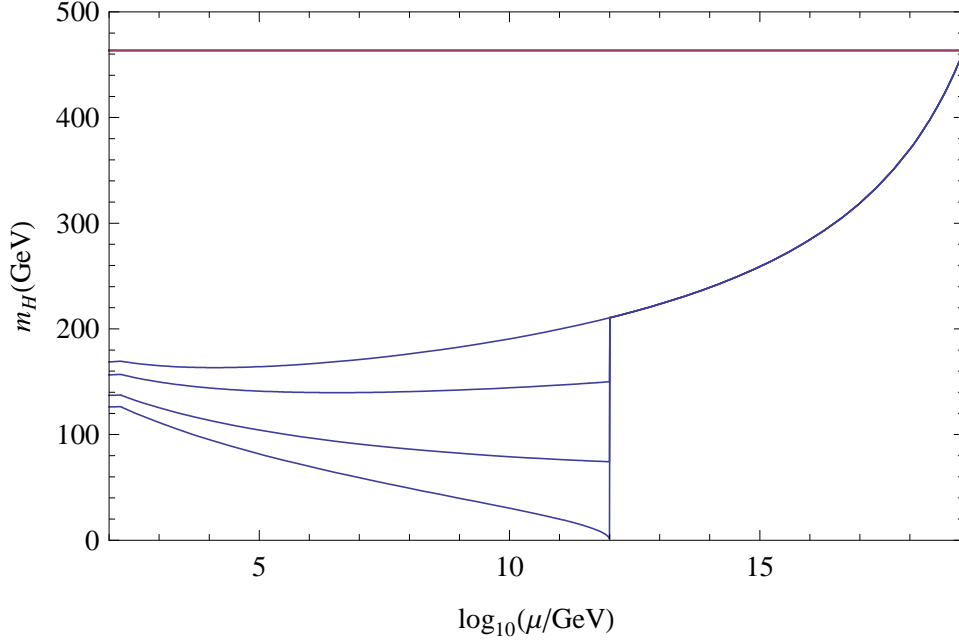


Figure 2: Evolution of running Higgs boson mass ($m_h(\mu = \sqrt{\lambda(\mu)}v)$) corresponding to the perturbativity bound for various λ_6 and $M_\Delta = 10^{12}$ GeV. Each line corresponds to $\lambda_6 = 0, 0.6, 0.8$ and 0.855 from top to bottom. The horizontal line corresponds to $M_H = (4\pi)^{1/4}v = 464$ GeV.

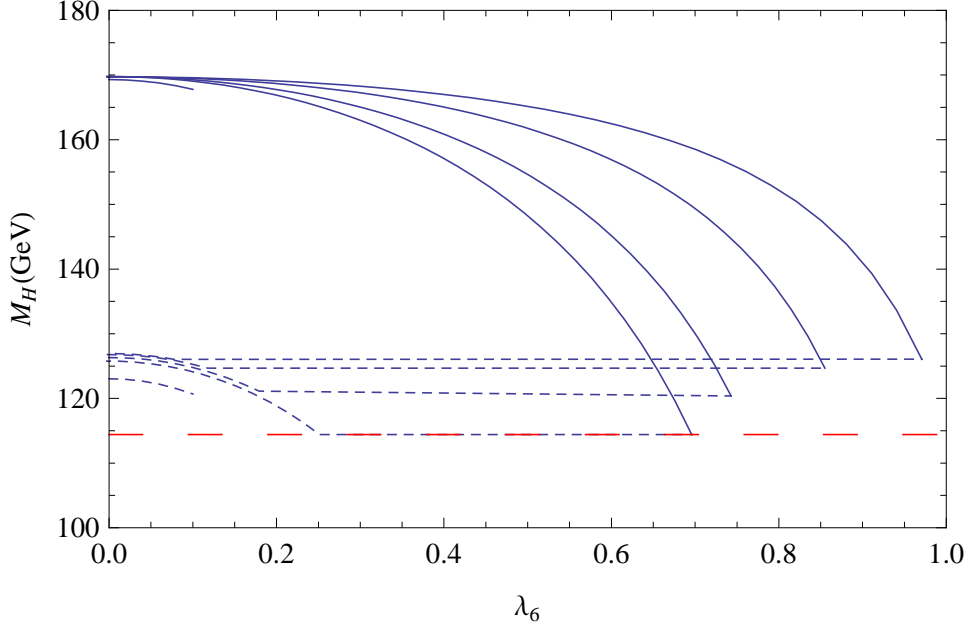


Figure 3: The perturbativity (solid) and vacuum stability (dotted) bounds on the Higgs boson pole mass M_H versus λ_6 for various M_Δ . Each solid and dashed lines correspond to $M_\Delta = 10^{14}$, 10^{12} , 10^9 , 1.14×10^7 and 10^3 GeV, from top to bottom. The results for $M_\Delta = 1$ TeV are shown only in the region $\lambda_6 \leq 0.1$ consistent with the ρ -parameter measurement. The dashed horizontal line denotes the LEP2 bound $M_H = 114.4$ GeV.

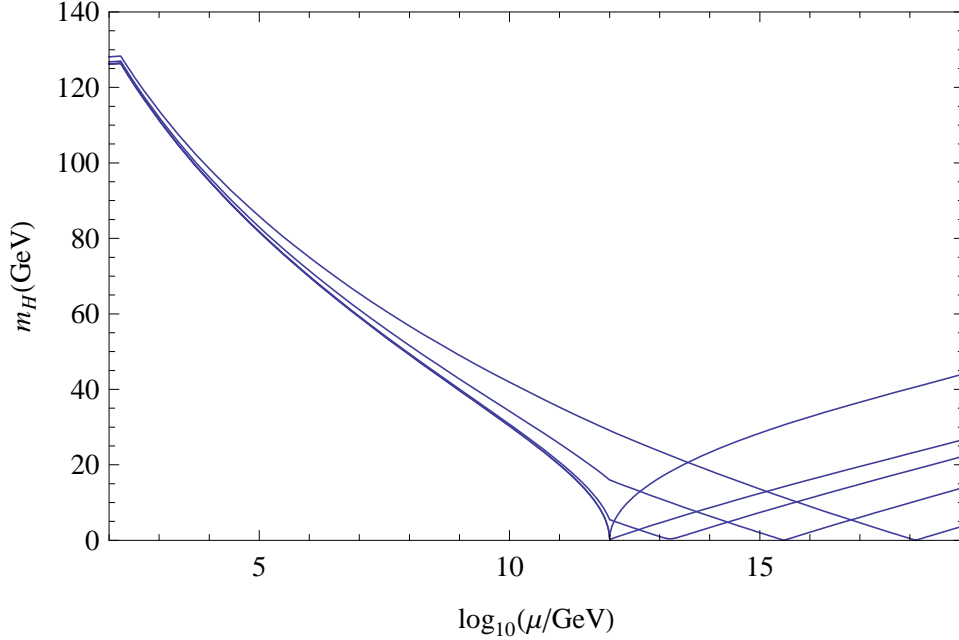


Figure 4: Evolution of running Higgs boson mass corresponding to the vacuum stability bound for various value λ_5 and $M_\Delta = 10^{12}$ GeV. Each line corresponds to $\lambda_5 = 0.3, 0.22, 0.2, 0.15$ and 0 , from top to bottom at $\log_{10}(\mu/\text{GeV}) = 19$.

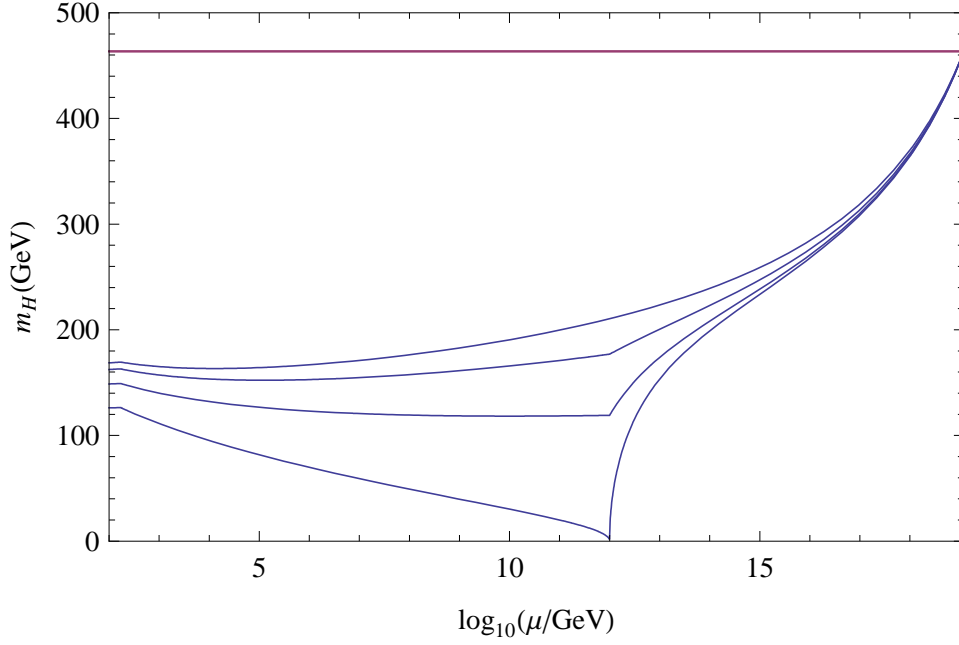


Figure 5: Evolution of running Higgs boson mass corresponding to the perturbativity bound for various λ_5 and $M_\Delta = 10^{12}$ GeV. Each line corresponds to $\lambda_5 = 0, 1.0, 1.25$ and 1.35 , from top to bottom. The horizontal line corresponds to $M_H = (4\pi)^{1/4}v = 464$ GeV.

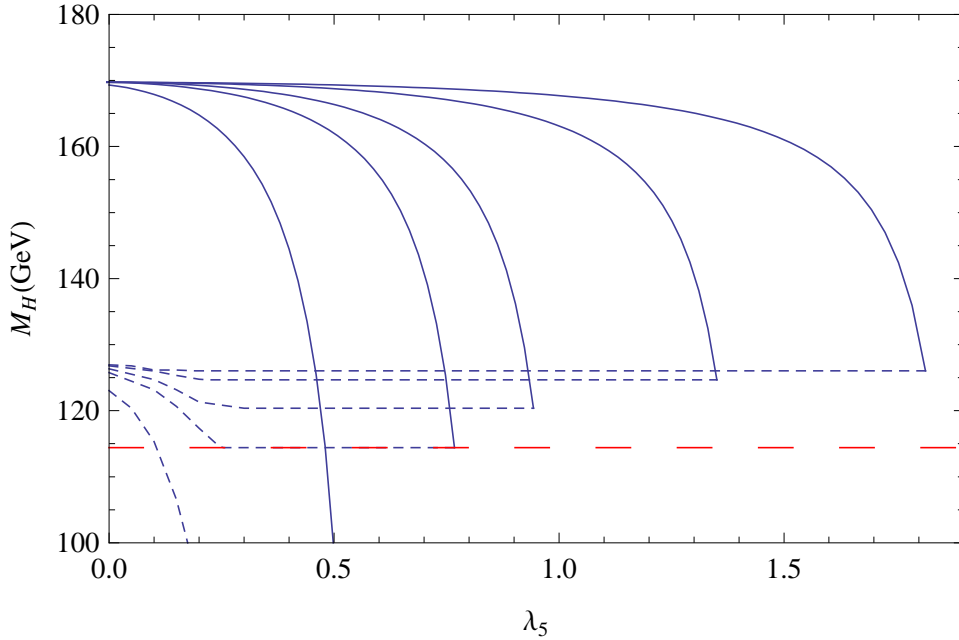


Figure 6: The perturbativity (solid) and vacuum stability (dotted) bounds versus λ_5 for various M_Δ . Each solid and dashed lines correspond to $M_\Delta = 10^{14}, 10^{12}, 10^9, 1.14 \times 10^7$ and 10^3 GeV, from top to bottom. The dashed horizontal line denotes the LEP2 bound $M_H = 114.4$ GeV.